Journal of Mines, Metals and Fuels, *70(9A) : 24-29; 2022. DOI: 10.18311/jmmf/2022/32246*

Print ISSN : 0022-2755

Journal of Mines, Metals and Fuels

Contents available at: www.informaticsjournals.com/index.php/jmmf

Study on the Various Parameters Affecting the Power Conversion Efficiency of Lead-Free Perovskite Solar Cell by SCAPS-1D

Rahul Kundara[1*] and Sarita Baghel[1]

[1] *Department of Applied Physics, Delhi Technological University, Bawana Road, Delhi-110042*

Abstract

Perovskite solar cells are becoming an alternative for conventional solar cells, attaining a performance of 29% approximately in eleven years (2009-2020). The SCAPS-1D was employed to take a look at the impact of various parameters inclusive of the thickness of the absorber layer, operating temperature, and defect density (Nt) on the performance of a perovskite solar cell (PSC). Two PSCs architectures are designed and simulated by adopting the SCAPS-1D. It is also employed to analyze the thin-film photovoltaic architecture. One model configuration is FTO/TiO_2/$CH_3NH_3SnI_3$/Cu_2O/Au and FTO/TiO_2/$CH_3NH_3GeI_3$/Cu2O/Au is the configuration of the second one. TiO_2 layer as electron transport layer (ETL) and Cu_2O layer used as hole transport layer (HTL) for both tin (Sn)-based and germanium (Ge)-based PSCs. The simulated result of both PSCs has been compared. In this study, careful theoretical optimization of photovoltaic (PV) parameters has also been done. This study examines the tolerance of Nt in the absorber layer. Optimized value of operating temperature, Nt, and thickness of perovskite layer for both the perovskite solar cells has been obtained using a simulation approach which leads to high PCE of a solar cell. By considering all optimized parameters $CH_3NH_3SnI_3$ PSC has achieved the maximum efficiency of 6.15 % and $CH_3NH_3GeI_3$ PSC has exhibited the highest PCE of 20.90 %. The results demonstrate that Sn and Ge-based PSCs are a future possibility to the PV device in terms of eco-friendly nature. This simulation works useful in the design of low-cost and high-efficiency lead-free PSC. These results will give the non-toxic and high-efficiency perovskite solar cell.

Keywords: *Parameters, power conversion efficiency, Perovskite solar cell, photovoltaic, SCAPS-1D, Renewable Simulation procedure, tolerance factor*

1. Introduction

The finite availability of nonrenewable resources and its severe effect on the environment is one of the causes of development of green and renewable energy resources. Biomass energy, solar energy and geothermal energy are examples of renewable energy sources. Solar energy has shown to be the best option for clean and sustainable energy resources. Due to its low cost and ecologically friendly production, perovskite solar cells are becoming a popular topic in thin-film photovoltaic research. A stable halide perovskite structure must have cations with suitable ionic size, as represented by geometrical constant t, is called as the tolerance factor and can be used as a measure of distortion of a perovskite from ideal cubic. The t ranges between 0.8 to 1.0 and the equation for tolerance factor is $t = (r_A + r_O)/ 2(r_B + r_O)$, where r_A, r_B, and r_O are ionic radii of A, B, and O, respectively [14]. Impact of various parameters on performance of a solar cell were studied such as thicknesses of perovskite, N_t and operating temperature. The solar cell simulation provided that the optimum value of thickness of $CH_3NH_3GeI_3$ absorber layer is approximately 600 nm. Ge-based PSCs with Cu_2O and DPBTTT-14 as HTM showed that overall PCE reached 21% [5]. It has been observed in simulation that performance of solar cells can be enhanced to some limit by changing the doping concentration and electron affinity of the buffer and HTM, whereas the deduction of

**Author for correspondence*

N_t of the absorber layer increases the solar cell efficiency. By optimizing the N_t of perovskite absorber layer, devices achieve great outcomes such as efficiency of 23.36% [7]. In planar heterojunction structure of Sn-based PSC, $CuSbS_2$ employed for the first time as HTL in combination with $MASnI_3$ absorber layer in this design because of its implicit features (high V_{OC}) than unstable and expensive Spiro-MeOTAD. By adoption of $CuSbS_2$ as a HTL in solar cell design, results are adequate with J_{SC} of 31.7 mA/cm^2, V_{OC} of 0.936 V, FF of 81.1% and maximum PCE of 24.1% [16]. The simulation was done and the device achieved results with V_{OC} of 0.5803 V, J_{SC} of 28.42 mA/cm^2, FF 45.41%, and maximum efficiency of 7.49% for $CH_3NH_3SnI_3$ [19]. Germanium based PSC with Cu_2O as HTM achieved a remarkable overall PCE of 21% [5]. In this study the simulated PSCs have shown different variation in their PV parameters with temperature, Nt and thickness. In Ge-based PSC the PCE increases with increase of thickness whereas in tin-based PSC the PCE decreases with increase of thickness, the PCE of both PSCs decrease with increase in temperature and PCE of both the PSCs decrease for increase in N_t. This is an excellent piece of work that shows that lead free PSCs can achieve performance levels similar to Pb-based PSC. An analysis of impact of variation in thickness of absorber layer, temperature which ranges between 300-480 K and variation in N_t of absorber layer also has been done.

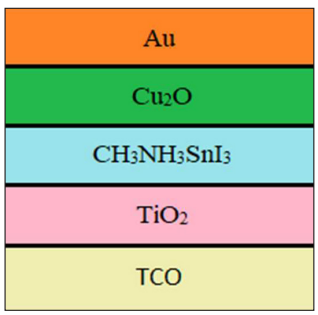

Fig. 1: Structure of the Simulated model of $CH_3NH_3SnI_3$ PSC

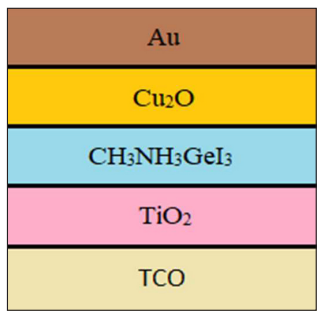

Fig. 2: Structure of the Simulated model of $CH_3NH_3GeI_3$ PSC

2. Simulation Procedure and Device Architecture

In this investigation, the 1D solar cell capacitance simulator SCAPS (version 3.3.10) has been employed for simulation. Gent University of Belgium developed SCAPS simulation software, which allows users to simulate up to seven semiconducting layers in both light and dark conditions [13]. This software can be used for simulations at different input physical conditions. This perovskite solar cell structure is formed with $CH_3NH_3SnI_3$ perovskite material with layer architecture as shown in Fig. 1: glass substrate/TCO/TiO_2/$CH_3NH_3SnI_3$/Cu_2O/Au-Metal and other PSC consist of $CH_3NH_3GeI_3$ absorber material with layer architecture as shown in Fig. 2: glass substrate/TCO/ TiO_2/$CH_3NH_3GeI_3$/Cu_2O/Au-Metal. The TCO layer in the structure is FTO. The input parameters employed in simulation of all layers are enclosed in Tables 1 and 2. The data of different parameters are chosen based on past experimental and theoretical studies [1-12]. The simulations were run at 300 K using a "air mass 1.5 global" spectrum and a light power of 1000 W/m^2. The work is dependent or related to variation in thickness of absorber layer, N_t of absorber layer, and operating temperature at which simulation of the proposed solar cell has been done. The performance of the solar cell has been absorbed via I–V characteristics of the solar cell which represents the following PV parameters: J_{SC}, FF, V_{OC}, and PCE. Procedure of simulation shown in Fig.3. All the input data used in SCAPS simulation obtained from experimental and theoretical work enclosed in Tables 1 and 2 for $CH_3NH_3SnI_3$ (cell-1) and $CH_3NH_3GeI_3$ (cell-2) respectively.

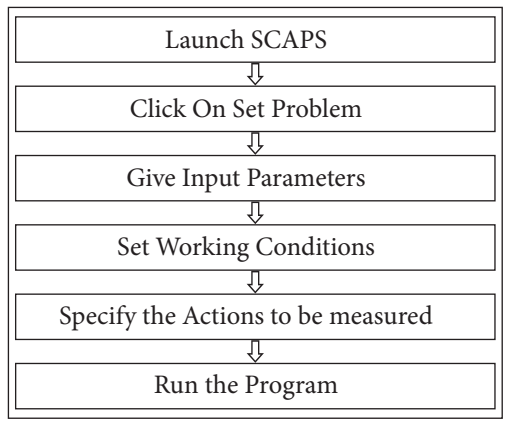

Fig. 3: SCAPS-1D software simulation procedure

Table 1. Various parameters employed in simulation (cell 1)

Parameter	FTO [11]	TiO_2 [7]	$CH_3NH_3SnI_3$ [8,9,10]	Cu_2O [12]
Thickness (μm)	0.5	0.03	0.345	0.350
Eg (eV)	3.5	3.2	1.3	2.17
χ (eV)	4.0	4.26 [8]	4.1	3.2
ε	9.0	9.0	8.2	7.11
N_C (cm^{-3})	2.2×10^{18}	2.0×10^{18}	10^{18}	2.02×10^{17}
N_V (cm^{-3})	1.8×10^{19}	1.8×10^{19}	10^{18}	1.1×10^{19}
μ_n (cm^2/Vs)	20	20	1.6	200
μ_p (cm^2/Vs)	10	10	1.6	80
N_D (cm^{-3})	1×10^{18}	1×10^{16}	-	0
N_A (cm^{-3})	0	0	1×10^{15}	1×10^{18}
N_t (cm^{-3})	-	1×10^{15}	4.5×10^{17}	1×10^{14}

Table 2. Various parameters used for simulation (cell 2)

Parameter	FTO [1,2]	TiO_2 [6]	$CH_3NH_3GeI_3$ [5]	Cu_2O [12]
Thickness (μ_m)	0.400	0.100	0.400	0.350
E_g (eV)	3.5	3.26	1.9	2.17
χ (eV)	4.0	4.2	3.98	3.2
ε	9.0	10	10	7.11
N_C (cm^{-3})	2.2×10^{18}	2.2×10^{18}	10^{16}	2.02×10^{17}
N_V (cm^{-3})	1.8×10^{18}	1.8×10^{19}	10^{16}	1.1 ×1019
μ_n (cm^2/Vs)	20	100	162×10^3	200
μ_p (cm^2/Vs)	10	25	101×10^3	80
N_D (cm^{-3})	1×10^{19}	1×10^{19}	109	0
N_A (cm^{-3})	0	-	109	1×10^{18}
N_t (cm^{-3})	-	-	10^{14}	1×10^{14}

3. Result and Discussion

3.1 Effect of change in thickness

The thickness of $CH_3NH_3SnI_3$ layer has exhibited a straight relation with evaluation of performance of PSC through its effect on charge carrier's diffusion length. It is known to us that as the thickness of the layer decreases, the absorption rate also decreases. This results in a decrease in photocurrent and therefore PCE of the solar cell also reduces from 200-1200 nm. Both J_{SC} and PCE parameters decrease exponentially for enlargement in the thickness from 200 to 1200 nm. The maximum efficiency of PSC goes up to 15.83% together with V_{OC} is 0.78 V, J_{SC} is 27.05 mA/cm^2 and FF is 74.8% for 200nm. The FF shows a monotonic decrease with the rise in thickness and also heads for enhancement gradually when thickness greater than 700nm [17]. In this work maximum efficiency of 7.64% has been achieved at 200 nm thickness of $CH_3NH_3SnI_3$ layer and 23.55% of PCE at the thickness of 1200nm for $CH_3NH_3GeI_3$ layer shown in Fig.4. The change in other PV parameters shown in Fig.4 with the help of Tables 3 and 4.

Table 3. Change in PV parameters with thickness of $CH_3NH_3SnI_3$ layer at 300 K and $N_t = 4.5 \times 10^{17}$ cm^{-3}.

Thickness (nm)	V_{oc} (V)	J_{sc} (mA/cm^2)	FF (%)	PCE (%)
200	0.6968	20.38	53.82	7.64
300	0.6869	19.72	48.73	6.60
400	0.6817	18.27	46.37	5.78
500	0.6789	17.04	45.39	5.25
600	0.6775	16.16	45.20	4.95
700	0.6769	15.58	45.43	4.79
800	0.6766	15.21	45.77	4.71
900	0.6765	15.00	46.07	4.68
1000	0.6765	14.89	46.25	4.66
1100	0.6765	14.83	46.34	4.65
1200	0.6765	14.80	46.37	4.64

Table 4. Variation in PV parameters with thickness of $CH_3NH_3GeI_3$ layer at 300 K and Nt = 10^{14} cm^{-3}.

Thickness (nm)	V_{oc} (V)	J_{sc} (mA/cm^2)	FF (%)	PCE (%)
200	1.8913	11.72	74.49	16.51
300	1.8769	13.05	78.16	19.16
400	1.8654	13.99	80.04	20.90
500	1.8559	14.67	80.56	21.94
600	1.8477	15.16	80.53	22.57
700	1.8406	15.53	80.28	22.96
800	1.8342	15.82	79.97	23.21
900	1.8284	16.04	79.65	23.36
1000	1.8232	16.21	79.33	23.46
1100	1.8185	16.36	79.05	23.52
1200	1.8140	16.47	78.80	23.55

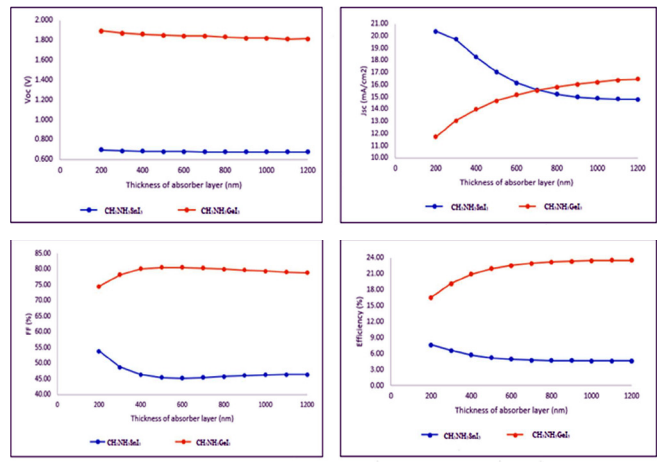

Fig.4: Impact of thickness on PV parameters of $CH_3NH_3SnI_3$ and $CH_3NH_3GeI_3$ PSCs

3.2 Effect of variation in operating temperature

To examine the effect of temperature at the efficiency of solar cells, operating temperature has been changed in the range of 300 to 480 K. Decline in the performance with temperature increase is related to decrease in diffusion length of charge carriers. Several solar cell architectures show instability of their overall performance because of deformation among layers at high temperature. When the temperature increases, the PCE drops significantly from 24.81% (at 300 K) to 17.05% (at 480 K) [17]. We have obtained maximum efficiency of 21.04% for $CH_3NH_3GeI_3$ PSC at the operating temperature of 340 K and the maximum PCE is 6.15% for $CH_3NH_3SnI_3$ PSC at operating temperature of 300 K shown below in Fig.5. VOC is decreasing with increase in the operating temperature for both PSCs. The impact of operating temperature on other PV parameters together with V_{oc}, J_{sc} and FF shown below in Fig.5 using Tables 5 and 6.

Table 5. Change in PV parameters with temperature of a $CH_3NH_3SnI_3$ PSC at 350 nm thickness and Nt = 4.5×10^{17} cm^{-3}.

Temperature (K)	V_{oc} (V)	J_{sc} (mA/cm^2)	FF (%)	PCE (%)
300	0.6839	19.00	47.31	6.15
320	0.6360	18.75	47.01	5.61
340	0.5876	18.46	46.59	5.06
360	0.5390	18.13	46.06	4.50
380	0.4900	17.75	45.43	3.95
400	0.4409	17.33	44.62	3.41
420	0.3916	16.89	43.62	2.89
440	0.3425	16.48	42.31	2.39
460	0.2939	16.11	40.66	1.93
480	0.2464	15.80	38.73	1.51

Table 6. Change in PV parameters with temperature of a $CH_3NH_3GeI_3$ PSC at 400 nm thickness and Nt = 10^{14} cm^{-3}.

Temperature (K)	V_{oc} (V)	J_{sc} (mA/cm^2)	FF (%)	PCE (%)
280	1.8752	13.96	79.34	20.78
300	1.8654	13.99	80.04	20.90
320	1.8527	14.02	80.80	21.00
340	1.8336	14.04	81.66	21.04
360	1.8040	14.06	82.70	20.99
380	1.7630	14.08	84.03	20.87
400	1.7175	14.09	85.37	20.67
420	1.6752	14.11	86.43	20.43
440	1.6386	14.11	87.04	20.14
460	1.6062	14.12	87.22	19.79
480	1.5766	14.13	87.16	19.42

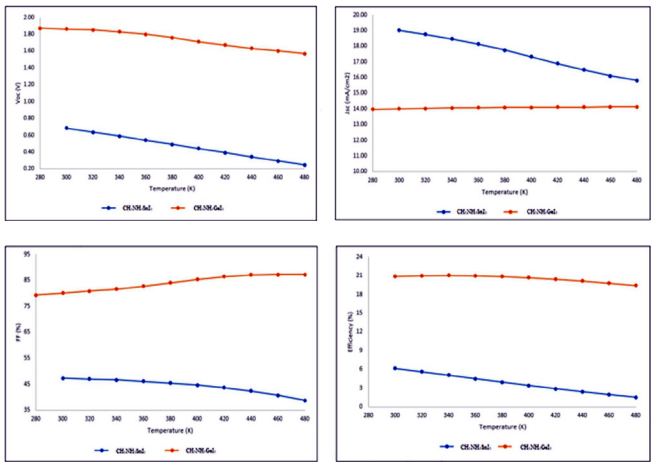

Fig.5: Change in the PV parameters of $CH_3NH_3SnI_3$ and $CH_3NH_3GeI_3$ PSCs with operating temperature

3.3 Impact of change in defect density

For $CH_3NH_3SnI_3$ perovskite layer when defect density increased, the unwanted recombination rate increased as the defects formed the dangling bonds, which behave as the trap state for the photo-generated charge carriers. Because of this short circuit current decreased, which is lastly responsible for decreasing FF of solar devices. The device PCE also decreased from 24.5% to 16.17%, when amphoteric Nt was enhanced from 10^{13} to 10^{17} cm^{-3}. Such an increasing amount of recombination resulted in a sharp fall in solar cell efficiency [18]. The optimized defect density is 4.5×10^{13} cm^{-3} for $CH_3NH_3SnI_3$ perovskite layer at which it has achieved the maximum efficiency of 24.18% shown in Fig. 6 and $CH_3NH_3GeI_3$ perovskite layer has achieved the highest PCE of 22.91% at which the defect density is 10^{13} cm^{-3} demonstrated in Fig. 7. The change in different PV parameters V_{oc}, J_{sc} and FF with defect density for $CH_3NH_3SnI_3$ PSC shown in Fig. 6 by using Table 7. For $CH_3NH_3GeI_3$ PSC the effect of Nt on PV parameters is demonstrated in Fig. 7 with the help of Table 8.

Table 7. Change in PV parameters with Nt of a $CH_3NH_3SnI_3$ PSC at 300 K and 350 nm thickness.

N_t (cm^{-3})	V_{oc} (V)	J_{sc} (mA/cm^2)	FF (%)	PCE (%)
4.5×1013	-	30.27	-	24.18
4.5×1014	6.5471	30.25	12.04	23.85
4.5×1015	1.3627	30.09	51.36	21.06
4.5×1016	0.8149	28.53	64.22	14.93
4.5×1017	0.6839	19.00	47.31	6.15

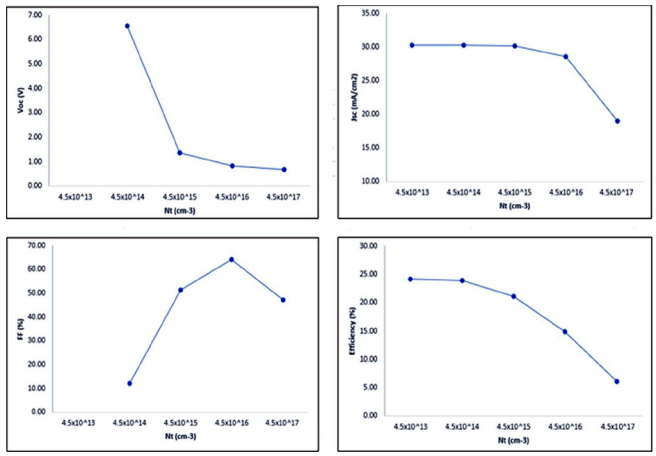

Fig.6: Impact of N_t on the performance of $CH_3NH_3SnI_3$ PSC

Table 8. Change in PV parameters with Nt of a $CH_3NH_3GeI_3$ PSC at 300 K and 400 nm thickness.

N_t (cm^{-3})	V_{oc} (V)	J_{sc} (mA/cm^2)	FF (%)	PCE (%)
1013	1.9617	13.999174	83.42	22.91
1014	1.8654	13.999174	80.04	20.90
1015	1.7674	13.999173	77.11	19.08
1016	1.6659	13.999170	76.14	17.76
1017	1.6154	13.999140	73.87	16.71

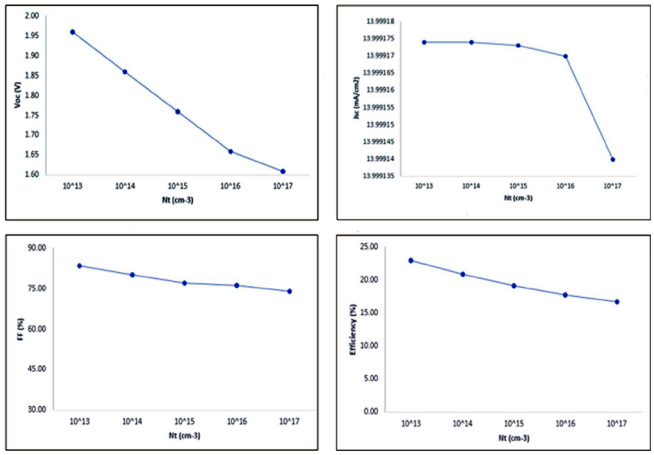

Fig. 7: Impact of N_t on the performance of $CH_3NH_3GeI_3$ PSC

Table 9. Device output of previous reported theoretical studies and outcome of present simulation for both PSCs.

$CH_3NH_3SnI_3$		
Parameter	**Simulation Reports [19]**	**Present Simulation**
V_{OC} (V)	0.58	0.68
J_{SC} (mA/cm^2)	28.42	19.00
FF (%)	45.41	47.31
PCE (%)	7.49	6.15

$CH_3NH_3GeI_3$		
Parameter	**Simulation Reports [5]**	**Present Simulation**
V_{OC} (V)	1.92	1.86
J_{SC} (mA/cm^2)	14.20	13.99
FF (%)	79.28	80.04
PCE (%)	21.60	20.90

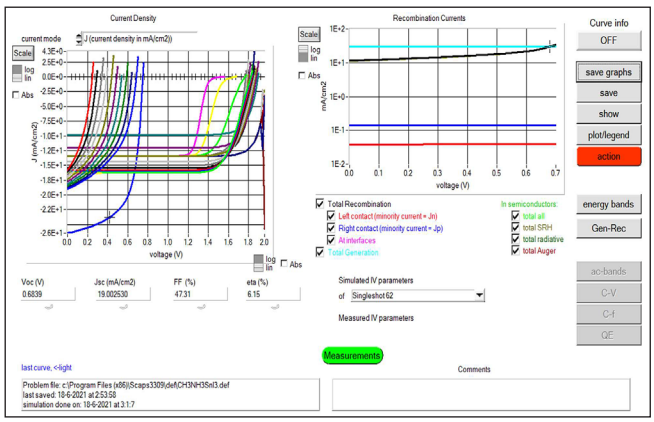

Fig. 8: Simulation outcome of $CH_3NH_3SnI_3$ based perovskite solar cell

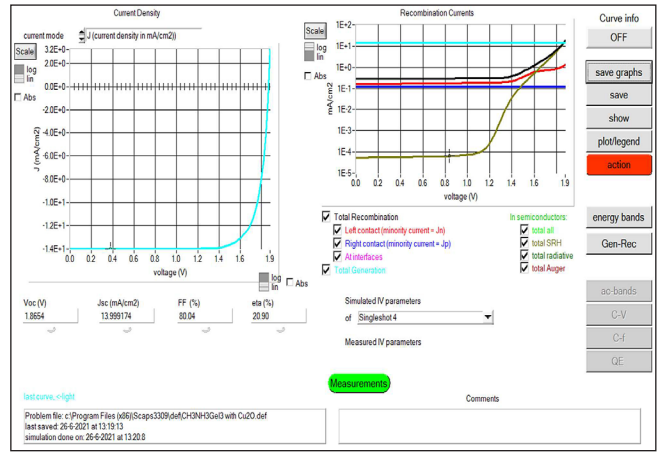

Fig. 9: Simulation outcome of $CH_3NH_3GeI_3$ based perovskite solar cell

4. Conclusions

This study optimized various parameters of PSC using SCAPS-1D software. The performance of these PSCs was found comparable to lead-based PSC. We have examined the impact of operating temperature, thickness, and N_t of both PSCs. The simulation was performed on the cell architecture of FTO/TiO_2/absorber layer/Cu_2O/Au. The optimized value of absorber layer thickness is 200 nm for $CH_3NH_3SnI_3$ and 1200 nm for $CH_3NH_3GeI_3$ perovskite solar cell. The optimal value of operating temperature is 300 K for Sn-based PSC and 340 K for Ge-based PSC. The optimized defect density value of Sn-based PSC is 4.5×10^{13} cm^{-13} and 10^{13} cm^{-3} for Ge-based PSC. The optimum value of operating temperature, thickness, and N_t is helpful in the fabrication of high PCE solar cells. It was observed that Ge-based PSC exhibited comparatively high performance. The maximum PCE of 20.90% was obtained at 300 K with V_{OC} of 1.8654 V, FF is 80.04%, and J_{SC} is 13.9991 mA/cm^2 for Ge-based PSC. Whereas Sn-based perovskite has achieved the PCE 6.15% and other PV parameters such as V_{OC} of 0.6839 V, FF 47.31%, J_{SC} is 19.0025 mA/cm^2 by employing SCAPS-1D. The simulation results provide the best approach for higher PCE solar cell device fabrication. We have observed that N_t, thickness, and the operating temperature have a deleterious impact on PSCs up to a certain value. This work might provide vital guidance for solar cell device design and optimization of different PV parameters for PSCs.

5. References

1. Sobayel, K.; Akhtaruzzaman, M.; Rahman, K.S.; Ferdaous, M.T.; Al-Mutairi, Z.A.; Alharbi, H.F.; Alharthi, N.H.; Karim, M.R.; Hasmady, S.; Amin, N. A comprehensive defect study of tungsten disulfide (WS2) as electron transport layer in perovskite solar cells by numerical simulation. *Results Phys.* 2019, 12, 1097–1103. [CrossRef]
2. Sobayel, K.; Shahinuzzaman, M.; Amin, N.; Karim, M.R.; Dar, M.A.; Gul, R.; Alghoul, M.A.; Sopian, K.; Hasan, A.K.M.; Akhtaruzzaman, M. Efficiency enhancement of CIGS solar cell by WS2 as window layer through numerical modelling tool. *Sol. Energy* 2020, 207, 479–485. [CrossRef]
3. Baktash, A.; Amiri, O.; Sasani, A. Improve efficiency of perovskite solar cells by using magnesium doped ZnO and TiO_2 compact layers. *Superlattices Microstruct.* 2016, 93, 128–137. [CrossRef]
4. Mahjabin, S.; Haque, M.M.; Sobayel, K.; Jamal, M.S.; Islam, M.A.; Selvanathan, V.; Abdulaziz, A.K.; Alharbi, H.F.; Sopian, K.; Amin, N.; et al. Perceiving of Defect Tolerance in Perovskite Absorber Layer for Efficient Perovskite Solar Cell. *IEEE Access* 2020,8, 106346–106353. [CrossRef]
5. Kanoun AA, Kanoun MB, Merad AE, Goumri-Said S. Toward development of high-performance perovskite solar cells based on CH3NH3GeI3 using computational approach. *Solar Energy.* 2019 Apr 1;182:237-44.
6. G.Xosrovashvili, N.E.Gorji," Numerical analysis of TiO_2/Cu_2ZnSnS_4 nanostructured PV using SCAPS- 1D", *Journal of Modern Optics*, DOI:Org/10.1080/09500340.2013.827252, Vol.60, No.11, pp.936-940.
7. Du H-J, Wang W-C, Zhu J-Z (2016) Device simulation of lead-free $CH_3NH_3SnI_3$ perovskite solar cells with high efficiency. *J Chin Phys B* 25:108802
8. Noel NK, Stranks SD, Abate A, Wehrenfennig C, Guarnera S, Haghighirad A-A, Sadhanala A, Eperon GE, Pathak SK, Johnston MB, Petrozza A, Herz LM, Snaith HJ (2014) Leadfree organic-inorganic tin halide perovskites for photovoltaic applications. *Energy Environ Sci* 7:3061–3068
9. Stoumpos CC, Malliakas CD, Kanatzidis MG (2013) Semiconducting tin and lead iodide perovskites with organic cations: phase transitions, high mobilities, and near-infrared photoluminescent properties. *Inorg Chem* 52:9019–9038
10. Chen QY, Huang Y, Huang PR, Ma T, Cao C, He Y (2016) Electronegativity explanation on the efficiency-enhancing mechanism of the hybrid inorganic–organic perovskite ABX3 from first-principles study. *Chin Phys B* 25:27104
11. E. Karimi, S.M.B. Ghorashi, Investigation of the influence of different hole-transporting materials on the performance of perovskite solar cells, *Optik (Stuttg)*. (2017), https://doi.org/10.1016/j.ijleo.2016.10.122.
12. M.I. Hossain, F.H. Alharbi, N. Tabet, Copper oxide as inorganic hole transport material for lead halide perovskite based solar cells, *Sol. Energy*. 120 (2015) 370–380. https://doi.org/10.1016/j.solener.2015.07.040.
13. M. Burgelman, P. Nollet, S. Degrave, Modelling polycrystalline semiconductor solar cells, *Thin Solid Films* 361-362 (2000) 527–532, https://doi.org/10.1016/S0040-6090(99)00825-1.
14. Jong UG, Yu CJ, Kye YH, Choe YG, Hao W, Li S. First-principles study on structural, electronic, and optical properties of inorganic Ge-based halide perovskites. *Inorganic chemistry*. 2019 Mar 13;58(7):4134-40.
15. Ke W, Stoumpos CC, Kanatzidis MG. "Unleaded" perovskites: status quo and future prospects of tin-based perovskite solar cells. *Advanced Materials*. 2019 Nov;31(47):1803230.
16. Devi C, Mehra R. Device simulation of lead-free $MASnI_3$ solar cell with $CuSbS_2$ (copper antimony sulfide). *Journal of materials science.* 2019 Apr 15;54(7):5615-24.
17. Yasin S, Al Zoubi T, Moustafa M. Design and simulation of high efficiency lead-free heterostructure perovskite solar cell using SCAPS-1D. *Optik.* 2021 Mar 1;229:166258.
18. Islam S, Sobayel K, Al-Kahtani A, Islam MA, Muhammad G, Amin N, Shahiduzzaman M, Akhtaruzzaman M. Defect Study and Modelling of SnX3-Based Perovskite Solar Cells with SCAPS-1D. *Nanomaterials.* 2021 May;11(5):1218.
19. Kumar M, Kumar A, Raj A, Sati PC, Sahni M, Anshul A. Organic-inorganic perovskite-based solar cell designs for high conversion efficiency: A comparative study by SCAPS simulation. *Materials Today: Proceedings*. 2020 Dec 15.
20. Toshniwal A, Jariwala A, Kheraj V, Opanasyuk AS, Panchal CJ. Numerical simulation of tin based perovskite solar cell: effects of absorber parameters and hole transport materials. *Journal of Nano and Electronic Physics.* 2017 Jul 1; 9(3).